PRELIMINARY INVESTIGATION OF A SINGLE-SHAFT BRAYTON ROTATING UNIT DESIGNED FOR A 2- TO 10-KILOWATT SPACE POWER GENERATION SYSTEM

by Robert Y. Wong, Hugh A. Klassen,
Robert C. Evans, and Charles H. Winzig

Lewis Research Center
Cleveland, Ohio

1. Report No. NASA TM X-1869	2. Government Accession No.	3. Recipient's Catalog No.
4. Title and Subtitle PRELIMINARY INVESTIGATION OF A SINGLE-SHAFT BRAYTON ROTATING UNIT DESIGNED FOR A 2- TO 10-KILOWATT SPACE POWER GENERATION SYSTEM		5. Report Date October 1969
		6. Performing Organization Code
7. Author(s) Robert Y. Wong, Hugh A. Klassen, Robert C. Evans, and Charles H. Winzig		8. Performing Organization Report No. E-5130
9. Performing Organization Name and Address Lewis Research Center National Aeronautics and Space Administration Cleveland, Ohio 44135		10. Work Unit No. 120-27
		11. Contract or Grant No.
		13. Type of Report and Period Covered Technical Memorandum
12. Sponsoring Agency Name and Address National Aeronautics and Space Administration Washington, D.C. 20546		
		14. Sponsoring Agency Code

15. Supplementary Notes

16. Abstract

A 525-hour hot test at design thermal conditions was made. The results indicated (1) that the performance of the turbine, compressor, and alternator are close to design specifications, (2) no evidence of major design flaws, (3) that the gas bearings had no short term operational problems, and (4) that alternator armature winding temperatures were higher than anticipated.

17. Key Words (Suggested by Author(s)) Brayton rotating unit Power generation system	18. Distribution Statement Unclassified - unlimited		
19. Security Classif. (of this report) Unclassified	20. Security Classif. (of this page) Unclassified	21. No. of Pages 39	22. Price* $3.00

CONTENTS

PRELIMINARY INVESTIGATION OF A SINGLE-SHAFT BRAYTON
ROTATING UNIT DESIGNED FOR A 2- TO 10-KILOWATT
SPACE POWER GENERATION SYSTEM

by Robert Y. Wong, Hugh A. Klassen, Robert C. Evans, and Charles H. Winzig

Lewis Research Center

SUMMARY

As part of an investigation into the application of the Brayton cycle to space electric power generation systems, a single-shaft turbine-compressor-alternator package designed for operation on gas bearings has been under investigation at the Lewis Research Center. The first phase of the hot testing of this machine, designated as the Brayton Rotating Unit or BRU, consisted of a total of 525 hours running at approximately design thermal conditions. The purpose of this test was threefold: (1) to verify the integrity of the design to withstand the required thermal conditions, (2) to verify in a gross sense the performance of the components, and (3) to gain assurance that there are no short term problems associated with the gas bearing operation. The results of the test showed that the performance of the turbine, compressor, and alternator were close to design specifications, that the subject machine operated for the 525 hours at approximately design thermal conditions without evidence of major design flaws, and that the gas bearings operated at approximately design thermal conditions for the 525 hours without deterioration in performance. Alternator armature winding temperatures were higher than anticipated.

INTRODUCTION

The NASA Lewis Research Center is investigating the application of the Brayton cycle to space electric power generation. As part of this program, a single-shaft turbine-compressor-alternator package, designated the Brayton Rotating Unit (BRU), was designed and manufactured under contract by the AiResearch Mfg. Co. of Arizona. Recently, units of this design have been delivered to the Lewis Research Center for experimental study and testing is currently in progress.

Reference 1 describes the space power system for which the BRU was designed. The system was specified to use a mixture of helium and xenon as the working fluid because of the good heat transfer properties of the mixture (see ref. 2). A molecular weight of 83.8 for the mixture was specifically chosen to be the same as krypton so that the aerodynamic properties such as flow rate, equivalent speed, compressor pressure ratio, and specific work would be identical for both fluids. Thus krypton, which is much less costly than the mixture, can be used for the testing of the machine at the same mechanical speed as required by the mixture. The BRU was designed for operation on gas bearings with a turbine inlet temperature of 2060° R (1144 K) and a net electrical output of 2 to 10 kilowatts at 36 000 rpm.

The first phase of the BRU testing consisted of a total of 525 hours of operation at approximately design thermal conditions with a net power output of 4 to 6 kilowatts. Net power output is defined herein as gross alternator power minus power consumed by the field exciter. The purpose of this test was threefold: (1) to verify the integrity of the design to withstand the required thermal conditions, (2) to verify in a gross sense the performance of the components of this machine, and (3) to gain assurance that there are no short term problems associated with gas bearing operation.

This report presents findings obtained from the first 525 hours of operation in which the turbine inlet temperature was maintained at 1955° to 2009° R (1086 to 1116 K). Design turbine inlet temperature was not obtained because of heat loss from the piping between the heater and the turbine inlet and a limitation on heater wall temperature. The test was started with krypton as the working fluid and a net power output of about 6 kilowatts. After a total of 250 hours of operation on krypton, a switch over to argon as the working fluid was made because of leaks in the piping and a minor leak in the BRU. This change in working fluid did not interfere with the attainment of the original test objectives. Ample data had already been obtained on the aerodynamic performance of the turbomachinery in krypton. In addition, operation with argon provided a heat transfer coefficient closer to that of the design mixture and therefore would give internal temperatures closer to those that would be obtained with the mixture.

Test results presented in this report include starting characteristics, performance of the components of the package, the thermal conditions obtained while operating on krypton and argon, and bearing performance. Also included is a description of the BRU and the test apparatus.

BRU DESIGN CONDITIONS

Turbomachinery

The 6-kilowatt design operating conditions for the BRU turbomachinery are as follows:

Working fluid . . . . Helium-xenon mixture
Working fluid molecular weight 83.8
Mass flow rate, lb/sec (kg/sec)
    Turbine 0.748 (0.339)
    Compressor 0.756 (0.343)
Turbine inlet temperature, ^{O}R (K) 2060 (1144)
Turbine inlet pressure, psia (N/cm^2 abs) 25.8 (17.8)
Turbine total-to-static pressure ratio 1.75
Compressor inlet temperature, ^{O}R (K) 540 (300)
Compressor inlet total pressure, psia (N/cm^2 abs) 14.2 (9.79)
Compressor total pressure ratio 1.9
Shaft speed, rpm 36 000

The difference in turbine and compressor flow results from the fact that approximately 2 percent of compressor flow is bled into the bearing housing to maintain bearing ambient pressure.

Alternator

The 6-kilowatt design operating conditions for the alternator are as follows:

Power, kW 6.0
Power factor 0.85
Frequency, Hz 1200
Liquid coolant flow, lb/sec (kg/sec) 0.12 (0.054)

Gas Bearings

The 6-kilowatt design operating conditions for the gas bearings are as follows:

Lubricant . . . . Helium-xenon mixture
Ambient temperature, ^{O}R (K) 860 (478)
Ambient pressure, psia (N/cm^2 abs) 25.0 (17.2)
Bearing number, $\lambda = 6\mu\omega R^2/p_o c^2$, dimensionless 0.74

where

c   average radial clearance, ft; m

p_o ambient pressure, lb/ft^2 abs; N/m^2 abs

R   bearing radius, ft; m

μ lubricant viscosity, (lb)(sec)/ft^2; (N)(sec)/m^2

ω rotative speed, rad/sec

BRU DESCRIPTION

Figure 1 is a photograph of the BRU installed in the test facility. Figure 2 is a schematic of the BRU showing the salient features. The radial-inflow turbine rotor and centrifugal compressor impeller are mounted on opposite ends of a common shaft with the alternator rotor between the two. The two journal bearings are located just outboard of each end of the alternator rotor. The thrust bearing is between the compressor impeller and the compressor end journal bearing. Each journal bearing consists of three self-acting pivoted pads. The thrust bearing is capable of taking thrust in either direction and has two stator plates each of which has nine stepped self-acting pads on it. All bearings are lubricated with system working fluid. The bearings are externally pressurized during startup and shutdown. More complete descriptions of the major components are given in the following sections.

Turbine

A photograph of the turbine rotor is shown in figure 3. The rotor diameter is 4.978 inches (12.64 cm) at the inlet and 3.460 inches (8.79 cm) at the outlet. There are 11 rotor blades and 11 splitter blades. The associated stator has 13 vanes and is an integral part of the scroll. Aerodynamic design information, including velocity diagrams and surface velocity distributions, may be found in reference 3.

Compressor

A photograph of the compressor impeller is shown in figure 4. The impeller diameter is 2.60 inches (6.60 cm) at the inlet and 4.25 inches (10.80 cm) at the outlet. There are 15 vanes in the rotor and 17 vanes in the diffuser.

Alternator

A cross-sectional view of the alternator is shown in figure 5. The alternator is a three-phase radial gap, four-pole unit with a design frequency of 1200 hertz. The composite, modified Lundell rotor is made of Inconel 718 and 4340 steel. Output voltage is 120/208. The design maximum continuous rating is 12.6 kilovolt-amperes with a 0.85 power factor. The alternator stator is equipped with two independent cooling coils for redundant cooling of the BRU.

Journal Bearings

Each journal bearing has three self-acting pivoted pads. A photograph of these pads and pivots is shown in figure 6. The pivot location is 65 percent of the pad length from the leading edge. The pads are made of Rex 49 tool steel with a hardness of 60 to 65 Rockwell C. The pivot consists of a fully conforming sliding contact ball and socket, both made of tungsten carbide. For low speed operation, external pressurization is supplied through a hole in the pivot to a single orifice in each pad. The balls of two of the pivots in each bearing are rigidly mounted to the frame. The third ball is mounted to a frame through a flexible beam with a nominal spring rate of 2000 pounds per inch (357 kg/cm). When the BRU is assembled, shims are placed between the flexible beam and the frame so that the bearing pad is preloaded against the shaft. Hence, the shaft is clamped between the three pads. A low spring rate was used to accommodate small amounts of differential growth which tend to change bearing clearances. The growth can be due to thermal as well as centrifugal forces. Bearing ambient pressure is maintained by a bleed from the compressor discharge. The labyrinth seals are sized to limit this bleed to 2 percent of the compressor flow. Ambient pressure control is required to maintain adequate bearing film thicknesses.

Thrust Bearing

A photograph of the thrust bearing is shown in figure 7. The bearing is double acting with a flat plate thrust runner. Each thrust stator plate has nine self-acting stepped sectors. The thrust stator material is M-50 tool steel with a Rockwell C hardness of

62 to 64. Each land is provided with an orifice for external pressurization during startup and shutdown. The entire thrust bearing is mounted on a gimbal assembly for self-alignment purposes.

BRU Internal Temperature Control

Several methods are used to control the BRU internal temperature; they are the following:

(1) Coolant flow through the alternator coolant passages
(2) Gold and rhodium plated radiation shields to minimize radiant heat transfer from the turbine
(3) Copper heat shunts to reduce shaft thermal gradients
(4) Minimum cross-sectional areas to reduce heat flow to low temperature parts
(5) Shaft curvic couplings with high resistance to heat flow
(6) Use of the compressor rotor as a heat sink

APPARATUS

A schematic drawing of the hot test facility is shown in figure 8. The operating conditions for a 6-kilowatt net power output are shown. In addition to the BRU, the facility components include a heat source, heat sink, and auxiliary systems for alternator cooling, voltage and speed control, inventory control, injection starting and supplying external pressurizing gas to the bearings. There is no recuperator for recovering heat from the turbine exhaust. These various components are described in the following sections.

Heat Source

The main heat source consists of a 100-kilowatt heater and a 60-kilowatt heater in series. Both heaters have direct resistance nichrome heating elements located in the gas stream. Heating element temperatures are automatically controlled at temperatures up to 2260° R (1255 K). Trace heaters are installed on the piping between the 60-kilowatt heater and the turbine inlet to reduce heat loss from the working fluid.

Heak Sink

Heat is rejected in a two-stage cooler. The first stage, which is water cooled, reduces the gas temperature to approximately 570° R (317 K). The second stage is cooled with refrigerated liquid. A minimum temperature of 460° R (273 K) can be obtained. The second stage gas outlet temperature is controlled by mixing the refrigerated liquid with warm liquid from the cooler.

Alternator Coolant System

The alternator coolant system utilized Dow Corning 200 which is supplied at 530° R (294 K) to the alternator coolant coils at a flow rate of approximately 0.14 pound per second (0.054 kg/sec). Coolant outlet temperature is approximately 560° R (311 K) for a 6-kilowatt power output. The heat sink refrigeration system supplies refrigerated liquid to a heat exchanger to remove the heat from the Dow Corning 200.

Inventory Control System

The inventory control system removes gas from the loop and stores it in receiving tanks for injection starts and hydrostatic jacking. When the bearings are externally pressurized, it continuously removes gas from the loop to maintain a constant pressure at the cooler outlet. Because of the high cost of krypton and helium-xenon mixtures, a closed system is required. The inventory control system is included in figure 8.

Gas from the compressor inlet line passes through the inventory control valve to the suction of a diaphragm compressor. The compressor discharges into a high pressure storage tank which supplies the bearing storage tank and injection systems. Pressure in the bearing supply storage tank is reduced to 200 pounds per square inch gage (138 N/cm^2 gage) by a regulator.

Injection Starting System

The package rotor is accelerated to self-sustaining speed by introducing gas into the 100-kilowatt heater inlet. The gas passes through both heaters before reaching the turbine. The injection starting system is included in figure 8.

A flow control valve is located between the injection point and the compressor discharge. This valve is closed during injection to prevent back flow toward the compressor.

Injection flow rate is controlled by two valves. The regulator valve is set to control injection line pressure at the desired value. Injection is accomplished by opening the injection valve to a preset value corresponding to the desired flow rate. Injection is cut off by a pressure switch when a specified pressure is reached in the compressor inlet line. The flow control valve can be opened by the same pressure switch or it can be opened by a second pressure switch which is set for another pressure. During injection the compressor flow is recirculated by a partially open compressor bypass valve to prevent compressor surge. It is closed by the same pressure switch that stops the injection. Injection flow rate is measured with an orifice plate.

Bearing Jacking Gas System

The bearing jacking gas system provides external pressurization to the journal and thrust bearings at speeds below 30 000 rpm. This system is included in figure 8. Each bearing is supplied with 150 pounds per square inch absolute (103 N/cm^2 abs) of gas from a separate regulator which is closed off manually for hydrodynamic operation. An emergency pressure regulator is in parallel with the normal regulator. The two supplies are isolated by solenoid valves. During hydrodynamic operation, if the speed drops below 30 000 rpm, the solenoid valves open automatically to provide external pressurization.

Voltage-Regulator-Exciter and Speed Control Systems

The voltage-regulator-exciter (hereafter referred to as VRE) and speed control system regulates the alternator line to neutral voltage at approximately 120 volts and limits speed to between 36 000 and 37 000 rpm (depending on load on speed controller). The power consumption of the speed controller load bank is varied to control speed.

INSTRUMENTATION

Chromel-Alumel thermocouples were used to measure all temperatures. Strain gage pressure transducers were used to measure all pressures. Data on performance of the turbine and compressor were determined from measuring stations near their inlet and outlet flanges. Each station contained a bare-spike total temperature rake, static pressure taps, and total pressure probes.

The compressor weight flow was measured with a Venturi flowmeter upstream of the compressor inlet. Injection weight flow was measured with an orifice flowmeter.

Motions of the shaft and bearing components were measured with noncontact capaci-

tance probes. These probes were included in the BRU design. Four probes were used for shaft orbit motions. At each journal bearing the shaft orbit was determined by two probes located near the bearing 90° apart in a radial plane. Each probe was in the same axial plane with a probe at the other journal. Four probes were used to measure thrust plate motion. Three measured turbine thrust film thickness, and the fourth measured compressor thrust film thickness. Eight probes measured the motions of the leading edges of journal bearing pads. Two probes measured thrust bearing gimbal motions. Compressor and turbine bearing loads were each determined by a probe which measured the motions of the beam-type springs of the flexibly mounted pads. Sixteen of the capacitance probe outputs were monitored on dual beam oscilloscopes. All probe outputs were continuously recorded on an FM magnetic tape recorder. Speed was measured in the following ways:

(1) Two capacitance probes produced signals with frequencies proportional to rotative speed. Six equally spaced recesses on the shaft produced varying clearances between the probes and the shaft.

(2) Alternator output frequency was measured by a counter.

Loop data were recorded by high-speed automatic data recorders and processed through a digital computer. During starts, 50 data points were recorded at a rate of 2500 data points per second. These included temperatures, pressures, thrust bearing film thicknesses, and electrical data. For steady-state operation, 200 data points were recorded at a rate of 20 data points per second.

PROCEDURE

The loop was operated for 100 hours on krypton; then it was shut down to repair piping leaks. It was then operated for another 150 hours on krypton. At the end of this time, the use of krypton was discontinued because of increasing leaks to atmosphere. The leaks were principally in the piping with a small leak in the BRU. The loop operation was maintained by adding argon to make up the losses so that the composition gradually changed from 100 percent krypton to 100 percent argon. The loop was shut down as planned after a total of 525 hours of hot operation, which consisted of two continuous runs of 100 and 425 hours.

Conditions for the two closed system injection starts are shown in table I. High-speed transient data were taken both times. For steady-state operation, 265 data points were taken at 2-hour intervals. Approximate operating conditions are shown in table II. The speed controller was used for all tests. For the first 100 hours, the field was externally excited with a dc power supply. During the remaining time, the VRE was in operation.

RESULTS AND DISCUSSION

As indicated in the INTRODUCTION, the preliminary test, totaling 525 hours of hot operation, was made with the BRU while operating as part of a breadboard powerplant at approximately design thermal conditions and net power outputs from 4 to 6 kilowatts. The purpose of this test was to verify the integrity of the design under design thermal conditions, to verify in a gross sense the performance of the components of the BRU, and finally to gain assurance that there are no short term problems associated with gas bearing operation. The results of the test will be presented and discussed in four separate sections as follows: (1) start characteristics, (2) package performance, (3) thermal maps, and (4) bearing performance.

Start Characteristics

Although an investigation of the start characteristics of the subject machine was not a principal objective of the test, transient recordings of pressure, temperature, speed, flow rate, and valve positions during a typical start are presented in figure 9 since it is an important aspect of the loop operation.

Briefly, typical starts with the BRU are made as follows. The system is first preheated and evacuated to approximately 6 pounds per square inch absolute (4 N/cm^2 abs). Then the external pressurization is applied to all bearings. Nominally constant injection flow is introduced at the 100-kilowatt heater inlet with the flow control valve closed and the compressor bypass valve open to prevent compressor surge. When conditions for self-sustaining operation are established, the injection flow is cut off, the flow-control valve opened, and the compressor bypass valve closed. From figure 9(a) which shows the positions of the injection, flow control, and compressor by-pass valves as a function of time, it can be seen that the injection valve starts to open at 2.5 seconds and starts to close at 8.2 seconds. Further, it can be seen that the flow control valve starts to open at 7.8 seconds. These three times should be borne in mind when studying the plots of pressure, weight flow, and speed.

From inspection of figure 9(b) it can be seen that the injection flow starts to rise from 0 to 2.5 seconds. The injection flow rises to a value of 0.75 pound per second (0.34 kg/sec) of krypton and remains nominally constant over the injection period. Figures 9(c), (d), and (e) show that the pressure, rotor speed, and temperature begin to rise at 2.8 seconds. The lag in time between the start of injection and the rise in speed is caused by the fairly large capacitance between injection point and the turbine inlet. As the injection flow fills the system, the pressure rises. The rise in pressure at the turbine inlet is much faster than the rise in pressure in the other parts of the system. This is due to the capacitance in the system downstream of the turbine and to a difference in

10

density in the working fluid resulting from heat addition and removal by the heater and cooler.

At 7.9 seconds, or shortly after the flow control valve starts to open, the compressor outlet pressure starts to rise sharply (fig. 9(c)), and the turbine inlet pressure drops sharply. This is due to a portion of the injection flow bleeding back toward the compressor. Between 8.2 and 9.0 seconds, the injection flow and the compressor bypass are cut off. Self-sustaining operation appears to have been established at 9.0 seconds.

In response to the pressure difference across the turbine (fig. 9(c)), the rotor speed as shown in figure 9(d) rapidly increases from 0 to 23 600 rpm or about 65 percent of design mechanical speed. At 23 600 rpm self-sustaining operation is achieved and, with the addition of more heat at the turbine inlet (as shown in fig. 9(e)), the rotor speed increases (fig. 9(d)). It should be noted that, at 44.5 seconds at a speed of 33 100 rpm, there is a dip in the speed curve. This is caused by manual control of the compressor bypass valve (fig. 9(a)) to control speed. Curves of turbine blade jet speed ratio (fig. 9(f)) and percent of design equivalent speed for the turbine (fig. 9(g)) and compressor (fig. 9(h)) are also included as a matter of interest.

After a typical start as just described was made for the 500-hour test, the speed was brought up to 36 000 rpm and controlled automatically by the speed controller. The pressure conditions for 6-kilowatt operation were set, and the transition to self-acting operation in all bearings was made by closing off the jacking gas.

Package Performance

All of the preliminary runs on the subject machine were made with axial clearances which were increased in the turbine to 0.030 inch (0.076 cm) and in the compressor to 0.020 inch (0.051 cm). Design cold values of axial clearance are 0.017 inch (0.043 cm) for the turbine and 0.008 inch (0.020 cm) for the compressor. This was done for assurance against loss of axial clearance during cold checkout runs and unforeseen conditions during hot runs which might cause a rub and precipitate a bearing failure. It was estimated that a loss of about one point in efficiency of both the turbine and compressor would result from the increased axial clearances. Further, it was expected that a slight loss in flow capacity of the compressor would also occur.

Table III contains a comparison of design and actual operating conditions for krypton which covered the first 250 hours of testing and for argon which covered the remainder of the test. Since extremely accurate calibrations were not made of the transducers on this run, the performance of the turbine, compressor, and alternator were qualitatively arrived at in the following manner. From the table it can be seen that, for the krypton run, the turbine inlet temperature was 105° R (58 K) below design which reduces turbine specific work by about 5 percent. The actual turbine pressure ratio, however, is higher than

11

design which results in a gain in turbine specific work of about 5 percent which in turn offsets the loss due to the lower temperature.

The compressor on the other hand is operating at slightly closer to open-throttle conditions than design which reduces the specific work required by the compressor slightly. This reduction is mitigated by the loss in efficiency which accompanies the shift in operating point toward open-throttle conditions. The indicated compressor flow, however, is about 3 percent lower than design but is compensated somewhat by a slightly lower than design compressor bleed flow.

The conclusion to be drawn from these observations is that the power of the turbine and compressor are very close to the design values. With a net alternator output of 6 kilowatts for krypton operation, it was concluded that the efficiencies of all three components were close to design.

From table III, it can also be seen that the BRU performance was vastly different when argon was used as the working fluid. This is because the higher energy content of argon reduces the aerodynamic speed of the turbomachinery to about 70 percent of that of krypton when operating at the same mechanical speed. This reduction in aerodynamic speed reduced the compressor pressure ratio to 1.39. This resulted in a decrease in electrical net output. In order to maintain alternator output as high as possible the compressor inlet pressure was increased to 18.7 pounds per square inch absolute (12.9 N/cm^2 abs).

BRU Internal Temperatures

As part of the design procedure for the subject machine, predictions of internal temperature distributions were made by the contractor. Accurate thermal maps are essential because such factors as initial clearances between parts, thermal stresses, and material selection are dependent upon these maps. Figure 10 shows the location of all thermocouples in the package. Table IV lists the predicted and actual temperatures for these locations for operation with krypton and argon. For krypton operation the predicted values agree reasonably well with the actual values. The greatest discrepancies occur in the alternator armature windings at locations 3 to 8. The largest discrepancy is 171° F (95° C) which is in location 4. This discrepancy may not be as large as 171° F (95° C) because the contractor may have misidentified the thermocouples. If this is so, then the maximum discrepancy is only about 100° F (56° C). The measured maximum temperatures of 371° F (189° C), however, are not excessive at the 6-kilowatt power level since the armature windings were designed for continuous operation at 428° F (220° C). At higher power levels, such as 10 kilowatts, the maximum predicted armature temperature is near 400° F (204° C). If a similar error exists at this power level, excessive winding temperature may result in a reduced life expectancy for the BRU.

12

During the hot tests, the elastomer O-rings used to seal the flange that mounts the turbine scroll to the BRU housing broke down because of excessive heat. Presented in figure 11 is a photograph of one of the O-rings and spacer. There is an identical O-ring on the other side of the spacer. The dark area on the spacer around the O-ring indicates deterioration of the ring. Since the O-ring grooves are located deep within the flange, it was not possible to place thermocouples close enough to measure the temperature of the metal adjacent to the ring. After cooldown, a flow check was made of the leakage past the O-ring and it was found to be about 0.75 pound per day (0.34 kg/day) of krypton with the housing pressure close to the design value of 25.1 pounds per square inch absolute (17.3 N/cm^2 abs). Because of other leaks in the piping, it was not possible to determine what the leak rate was when it was hot. The BRU design provides for an alternate method of sealing the turbine scroll mounting flange. The O-ring seal was intended only for initial testing. In the future, the O-ring will be eliminated and the flange sealed by welding.

Removal of the turbine and compressor scrolls revealed some deterioration of the heat shielding. Some of the gold plating had fallen off because of defective plating and parts of the gold heat shield were blackened as shown in figure 12. Also, the turbine seal holder which is rhodium plated (fig. 2) had a white cloudy film as shown in figure 13. This indicates an increase in absorptivity of this surface.

During the 275-hour argon test, the temperature measured on the inside of the turbine seal holder increased by approximately 1.5 percent. This may be due to an increase in emissivity of the gold plated surface of the turbine inlet scroll and an increase in absorptivity of the rhodium plated surface on the turbine seal holder. However, the temperatures of the bearings, bearing carriers, alternator, and other components inboard from the turbine seal carrier did not increase noticeably. These components are protected by the copper heat shunt located between them and the turbine seal carrier (fig. 2). If the deterioration continues, some increase may occur in the temperatures of these components. It is not known whether all the plating deterioration is inherent in the BRU or if it could be caused by contaminants from the facility.

Bearing Component Motions

Photographs of the bearing component oscilloscope traces were taken approximately every 100 hours and a typical set is presented in figure 14. The photographs showed no changes with time in the peak-to-peak values of the traces or in the wave forms. Each small division of the grid is equal to 0.0001 inch (0.00025 cm).

The compressor bearing orbit is shown in figure 14(a). The orbit is slightly elliptical with a major axis of 0.00012 inch (0.00030 cm). The corresponding time base probe traces are shown in figure 14(b). Both waves are sinusoidal and less than 90° out of phase.

The turbine bearing orbit is shown in figure 14(c). The orbit is oval with a major axis of 0.00017 inch (0.00043 cm). The time base traces are shown in figure 14(d). The waves are roughly sinusoidal, with some distortion, and are more than 90° out of phase.

The top two traces of figure 14(e) show the motions of the corners of the leading edge of the turbine flexibly mounted pad. The amplitude for both corners is 0.00018 inch (0.00046 cm). The two waves are in phase, showing that the pad is moving with a plain pitching motion. The bottom two traces show the motions of the leading edge of one of the turbine solidly mounted pads. The magnitudes are 0.0001 inch (0.00025 cm) and 0.00008 inch (0.00020 cm). The leading edge movements of the solid mounted pad are smaller than for the flexibly mounted pad because the flexibly mounted pads have the radial translation of the pivot superimposed. The two waves are in phase, showing that this pad also has a plain pitching motion. The shape of both traces indicates that an extra excitation occurs during each cycle. This same type of motion was observed during previous tests and is discussed in reference 4. The shape of the trace is attributed to a sudden reversal in the direction of pad pitching motion.

The top trace in figure 14(f) shows the motion of one corner of the leading edge of the compressor flexibly mounted pad. This trace is similar to those for the turbine flexibly mounted pad. The magnitude is 0.00012 inch (0.00030 cm). The bottom trace shows the motion of one corner of a compressor solidly mounted pad. The motion is very small with a magnitude of about 0.00002 inch (0.00005 cm).

Figure 14(g) shows the radial motions of the turbine and compressor beam-sprung pivots. The top trace shows the turbine pivot motion. Both have a magnitude of about 0.00012 inch (0.00030 cm). The two traces are approximately 180° out of phase, indicating the geometric shaft axis is moving in a conical fashion.

Figure 14(h) shows the motions of the two opposite sides of the thrust runner. The top trace is the compressor side. The magnitudes are 0.00007 inch (0.00018 cm) for the compressor and 0.00010 inch (0.00025 cm) for the turbine. As expected, the two traces are about 180° out of phase.

Figure 14(i) shows the motions of the thrust gimbals. The top trace shows a magnitude of 0.00008 inch (0.00020 cm). Most of this is caused by a subsynchronous motion superimposed on the 600-hertz gimbal motion associated with rotational speed. The bottom trace has a magnitude of about 0.00002 inch (0.00005 cm).

The operation of these bearings in argon appears to be identical to that of krypton with the exception of indicated journal bearing load. The indicated journal bearing load for krypton was 5 to 6 pounds (2.3 to 2.7 kg) higher than for argon. The self-acting film pressure measured at the orifice indicated very close to the same pressure for both gases. Therefore, unless there are drastically different pressure distributions for the two gases, it is believed that the journal bearing loads for the two gases were about the same. Some unpublished data obtained experimentally with argon from bearings identical to the BRU but installed in the machine described in reference 5, indicated that journal bearing load

is between 0.75 and 0.8 of the pressure difference between the self-acting pressure in the film measured at the orifice and the bearing ambient pressure. This unpublished data would indicate a journal bearing load of approximately 14 pounds (6.4 kg) for both bearings as compared with indicated loads of 16 to 18 pounds (7.3 to 8.2 kg) during the argon test and 19 to 24 pounds (8.6 to 10.9 kg) during the krypton tests.

During the BRU start, the rotor acceleration was so rapid that the bearing motions going through the critical speed range were very small. The thrust load (as indicated by the thrust film thickness) imposed by the high pressure drop across the turbine rotor never became great enough to overcome the thrust load toward the compressor caused by the weight of the rotor.

SUMMARY OF RESULTS

The results of a preliminary 525-hour test on the subject Brayton Rotating Unit (BRU) operating as part of a breadboard powerplant at approximate design thermal conditions and 4- to 6-kilowatt net power output are summarized as follows:

1. The performance of the turbine, compressor, and alternator were found to be very close to design specifications.

2. The subject machine was operated for the total of 525 hours at approximately design thermal conditions without evidence of major design flaws.

3. The bearings operated at approximately design thermal condition for the total of 525 hours without deterioration in performance. This indicated that there are no major short term problems associated with gas bearing operation.

4. Some deterioration was noted in the gold and rhodium plating of heat shields. Continued deterioration may result in some increase in BRU internal temperatures.

5. Alternator armature winding temperatures were higher than anticipated.

Lewis Research Center,
National Aeronautics and Space Administration,
Cleveland, Ohio, July 21, 1969,
120-27.

REFERENCES

1. Klann, John L.: 2 to 10 Kilowatt Solar or Radioisotope Brayton Power System. Presented at the Intersociety Energy Conversion Engineering Conference, IEEE, Boulder, Colo., Aug. 14-16, 1968.

2. Vanco, Michael R.: Analytical Comparison of Relative Heat-Transfer Coefficients and Pressure Drops of Inert Gases and Their Binary Mixtures. NASA TN D-2677, 1965.

3. Nusbaum, William J.; and Kofskey, Milton G.: Cold Performance Evaluation of a 4.97-Inch Radial-Inflow Turbine Designed for Single-Shaft Brayton Cycle Space-Power System. NASA TN D-5090, 1969.

4. Wong, Robert Y.; Klassen, Hugh A.; Evans, Robert C.; and Spackman, Donald J.: Use of an Electronic Visualization Technique in the Study of Gas Journal Bearing Behavior. NASA TM X-1609, 1968.

5. Anon.: Design and Fabrication of a High-Performance Brayton Cycle Radial-Flow Gas Generator. NASA CR-706, 1967.

TABLE I. - INJECTION START CONDITIONS

System	1	2
Injection flow rate, lb/sec (kg/sec)	0.74 (0.34)	0.74 (0.34)
Turbine inlet temperature, ^{O}R (K)	1470 (817)	1360 (756)
Initial loop pressure, psia (N/cm^2 abs)	5.42 (3.74)	5.13 (3.54)
Injection cutoff pressure, psia (N/cm^2 abs)	13.0 (8.96)	13.0 (8.96)
Pressure for flow control valve opening, psia (N/cm^2 abs)	11.8 (8.14)	11.9 (8.21)

TABLE II. - TYPICAL OPERATING CONDITIONS

Time, hr	100	150	275
Working fluid	Krypton	Krypton	Argon
Turbine inlet temperature, ^{O}R (K)	1970 (1090)	1950 (1080)	2000 (1110)
Turbine inlet pressure, psia (N/cm^2 abs)	24.0 (16.5)	25.7 (17.7)	25.5 (17.6)
Turbine total pressure ratio	1.78	1.80	1.36
Alternator output, kW	5.9	6.1	4.6
Compressor inlet temperature, ^{O}R (K)	537 (298)	538 (299)	535 (297)

TABLE III. - COMPARISON OF 6-KILOWATT DESIGN AND ACTUAL OPERATING CONDITIONS

FOR TWO POINTS IN 525-HOUR TEST PERIOD

	Design	Krypton	Argon
Turbine inlet total pressure, psia (N/cm^2 abs)	25.8 (17.8)	25.8 (17.8)	25.8 (17.8)
Turbine inlet total temperature, ^{O}R (K)	2060 (1144)	1955 (1086)	2009 (1116)
Turbine outlet total pressure, psia (N/cm^2 abs)	14.7 (10.1)	14.2 (9.79)	18.8 (13.0)
Turbine total-to-total pressure ratio	1.75	1.80	1.36
Compressor inlet total pressure, psia (N/cm^2 abs)	14.2 (9.79)	14.0 (9.65)	18.7 (12.9)
Compressor inlet total temperature, ^{O}R (K)	540 (300)	540 (300)	535 (297)
Compressor outlet total pressure, psia (N/cm^2 abs)	27.0 (18.6)	26.2 (18.1)	26.1 (18.0)
Compressor total-to-total pressure ratio	1.90	1.86	1.39
Corrected compressor weight flow, lb/sec (kg/sec)	0.84 (0.38)	0.81 (0.37)	0.32 (0.15)
Compressor bleed flow, lb/sec (kg/sec)	0.016 (0.0072)	0.010 (0.0045)	0.0050 (0.0023)
Power output, kW	6	6	4.7
Speed, rpm	36 000	36 595	36 515

17

Working fluid	Krypton		Argon	
Operation condition	Design	Actual	Design	Actual
Turbine inlet pressure, psia (N/cm^2 abs)	25.81 (17.80)	25.81 (17.80)	(a)	25.7 (17.7)
Turbine inlet temperature, ^{O}R (K)	2060 (1144)	1955 (1086)	2060 (1144)	2009 (1116)
Compressor inlet pressure, psia (N/cm^2 abs)	14.21 (9.80)	14.01 (9.66)	(a)	18.7 (12.9)
Compressor inlet temperature, ^{O}R (K)	540 (300)	539.6 (299.8)	467 (259)	535 (297)
Power output, kW	6	6.1	6	4.7
Thermocouple	Temperature, ^{O}F (^{O}C)			
1	275 (135)	206 (96)	250 (121)	173 (79)
2	260 (127)	239 (115)	240 (116)	194 (90)
3	200 (93)	344 (173)	180 (82)	273 (134)
4	200 (93)	371 (189)	140 (60)	286 (141)
5	350 (177)	349 (176)	268 (131)	277 (136)
6	200 (93)	274 (134)	200 (93)	222 (105)
7	200 (93)	272 (133)	200 (93)	221 (105)
8	200 (93)	276 (135)	200 (93)	222 (105)
9	140 (60)	131 (55)	130 (54)	119 (48)
10	135 (57)	133 (54)	125 (52)	116 (47)
11	140 (60)	131 (55)	130 (54)	124 (51)
12	135 (57)	120 (49)	120 (49)	107 (42)
13	390 (199)	303 (151)	425 (219)	307 (153)
14	390 (199)	309 (154)	425 (219)	312 (155)
15	390 (199)	307 (153)	425 (219)	315 (157)
16	200 (93)	166 (74)	145 (63)	132 (55)
17	200 (93)	164 (73)	145 (63)	132 (55)
18	200 (93)	190 (88)	145 (63)	150 (66)
19	160 (71)	174 (79)	140 (60)	169 (76)
20	400 (204)	446 (229)	360 (182)	344 (173)
21	230 (110)	232 (111)	200 (93)	200 (93)
22	210 (99)	228 (108)	170 (77)	178 (81)
23	405 (207)	437 (225)	375 (191)	348 (175)
24	405 (207)	436 (224)	375 (191)	349 (176)
25	(a)	327 (164)	(a)	277 (136)
26	(a)	328 (164)	(a)	278 (136)
27	362 (183)	402 (205)	290 (143)	291 (144)
28	362 (183)	400 (204)	290 (143)	289 (143)
29	(a)	311 (155)	(a)	229 (109)
30	(a)	317 (158)	(a)	234 (112)
31	460 (238)	465 (241)	315 (157)	329 (165)
32	460 (238)	468 (242)	315 (157)	328 (164)
33	400 (204)	388 (197)	280 (138)	281 (139)
34	600 (316)	834 (445)	600 (316)	889 (476)
35	950 (510)	1052 (567)	1000 (538)	1132 (611)
36	950 (510)	976 (524)	1050 (566)	1036 (557)
37	225 (107)	238 (114)	190 (88)	219 (104)
38	---	---	---	---
39	278 (136)	254 (123)	107 (42)	164 (73)
40	278 (136)	276 (135)	107 (42)	175 (80)

[a]Not available because contractor did not calculate this.

TABLE IV. - Concluded. COMPARISON OF PREDICTED AND ACTUAL TEMPERATURE DISTRIBUTION

FOR OPERATION WITH KRYPTON AND ARGON

Working fluid	Krypton		Argon	
Operation condition	Design	Actual	Design	Actual
Turbine inlet pressure, psia (N/cm^2 abs)	25.81 (17.80)	25.81 (17.80)	(a)	25.7 (17.7)
Turbine inlet temperature, ^{O}R (K)	2060 (1144)	1955 (1086)	2060 (1144)	2009 (1116)
Compressor inlet pressure, psia (N/cm^2 abs)	14.21 (9.80)	14.01 (9.66)	(a)	18.7 (12.9)
Compressor inlet temperature, ^{O}R (K)	540 (300)	539.6 (299.8)	467 (259)	535 (297)
Power output, kW	6	6.1	6	4.7
Thermocouple	Temperature, ^{O}F (^{O}C)			
41	278 (136)	272 (133)	107 (42)	171 (78)
42	260 (127)	281 (139)	100 (38)	172 (78)
43	(a)	97 (36)	(a)	84 (29)
44	240 (116)	237 (114)	120 (49)	157 (70)
45	240 (116)	249 (121)	120 (49)	171 (78)
46	240 (116)	247 (120)	120 (49)	167 (75)
47	210 (99)	201 (94)	140 (60)	146 (63)
48	210 (99)	218 (103)	140 (60)	158 (70)
49	210 (99)	208 (97)	140 (60)	151 (67)
50	270 (132)	139 (59)	225 (107)	117 (47)
51	340 (171)	178 (81)	325 (163)	165 (74)
52	300 (149)	185 (85)	275 (135)	161 (72)
53	300 (149)	194 (90)	275 (135)	174 (79)
54	300 (149)	122 (50)	275 (135)	109 (43)
55	(a)	111 (44)	(a)	95 (35)
56	(a)	103 (40)	(a)	90 (32)
57	(a)	141 (61)	(a)	129 (54)
58	390 (199)	402 (205)	410 (210)	412 (211)
59	390 (199)	405 (207)	410 (210)	412 (211)
60	390 (199)	412 (211)	410 (210)	430 (221)
61	390 (199)	289 (198)	410 (210)	402 (205)
62	425 (219)	439 (226)	440 (227)	461 (239)
63	425 (219)	434 (223)	440 (227)	441 (228)
64	425 (219)	425 (219)	440 (227)	431 (222)
65	425 (219)	397 (203)	440 (227)	418 (214)
66	650 (343)	844 (451)	625 (330)	897 (481)
67	1000 (538)	1055 (569)	1000 (538)	1111 (600)
68	1300 (704)	1244 (673)	1450 (788)	1306 (707)
69	1300 (704)	1258 (681)	1450 (788)	1321 (717)
70	1300 (704)	1239 (670)	1450 (788)	1302 (706)
71 (Turbine inlet flange)	1600 (871)	1428 (775)	(a)	1484 (806)
72	1600 (871)	1424 (773)	(a)	1485 (807)
73	1600 (871)	1426 (774)	1550 (843)	1489 (809)
74	1550 (843)	1403 (762)	1550 (843)	1474 (801)
75	1550 (843)	1399 (759)	1550 (843)	1468 (797)
76	1550 (843)	1407 (764)	1550 (843)	1477 (803)

[a]Not available because contractor did not calculate this.
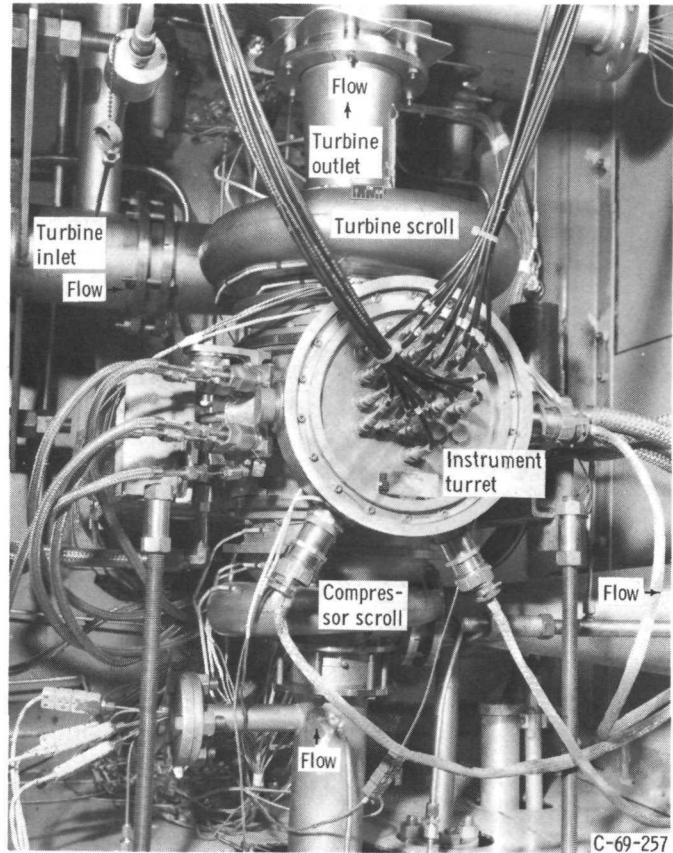
Figure 1. – Photograph of Brayton rotating unit (BRU).
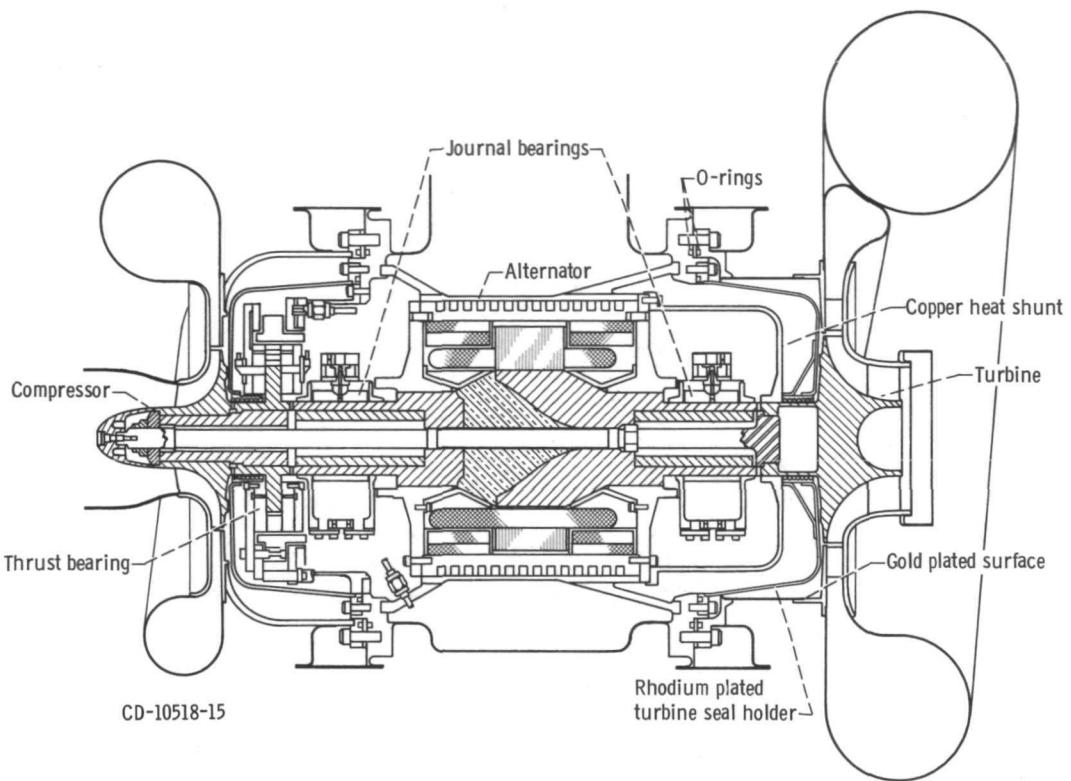
Figure 2. - Schematic of BRU.

CD-10518-15

Journal bearings
O-rings
Alternator
Copper heat shunt
Compressor
Turbine
Thrust bearing
Gold plated surface
Rhodium plated
turbine seal holder

C-69-1068
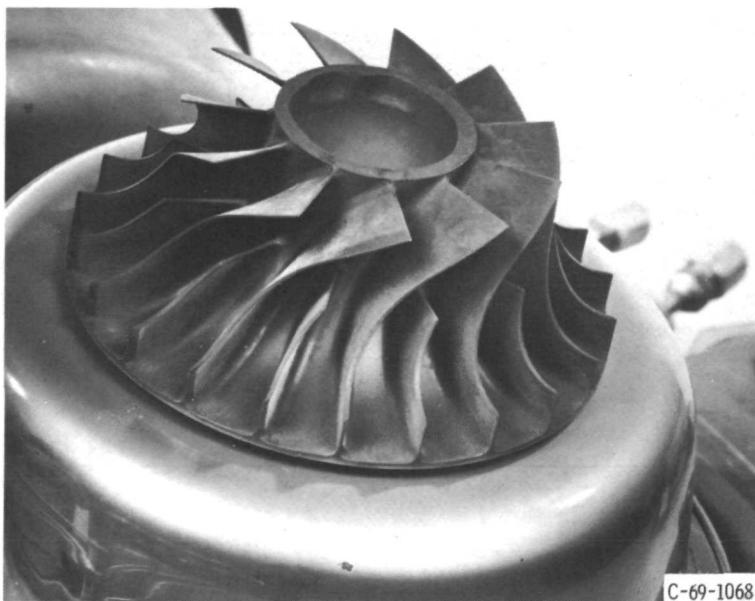
Figure 3. - Turbine wheel.
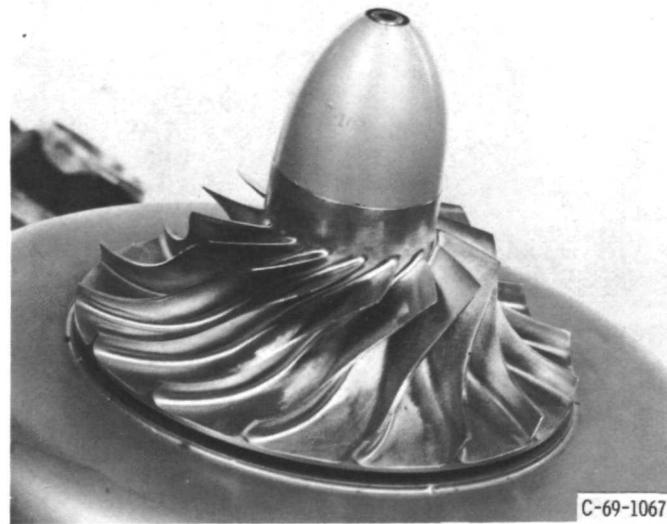
Figure 4. – Compressor impeller.
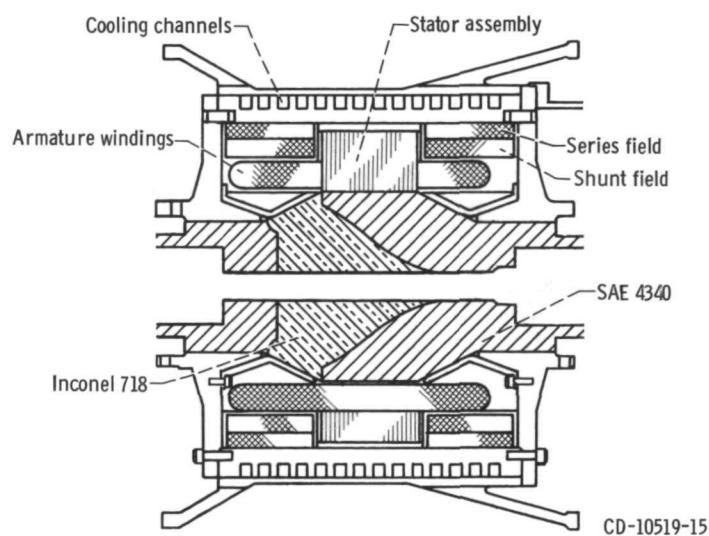

Figure 5. – Sectional view of BRU alternator.

Bearing carrier

Pad

Pivot

C-69-2097
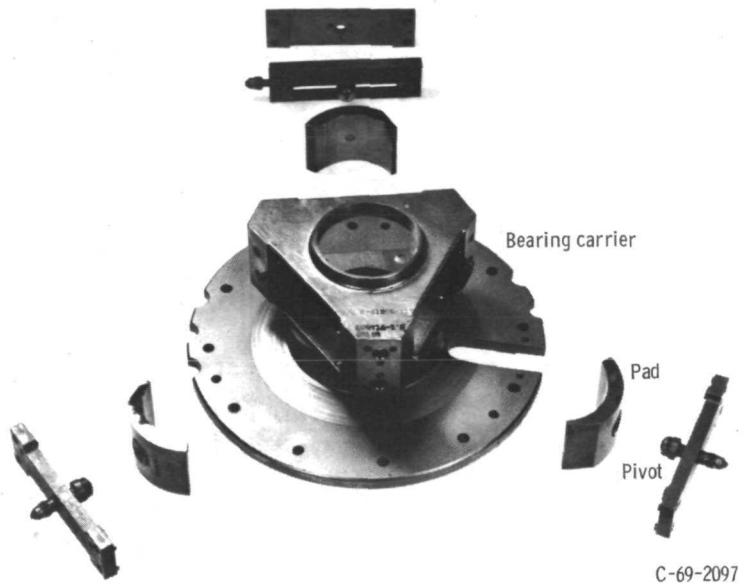
Figure 6. - Journal bearing assembly.

C-69-2098
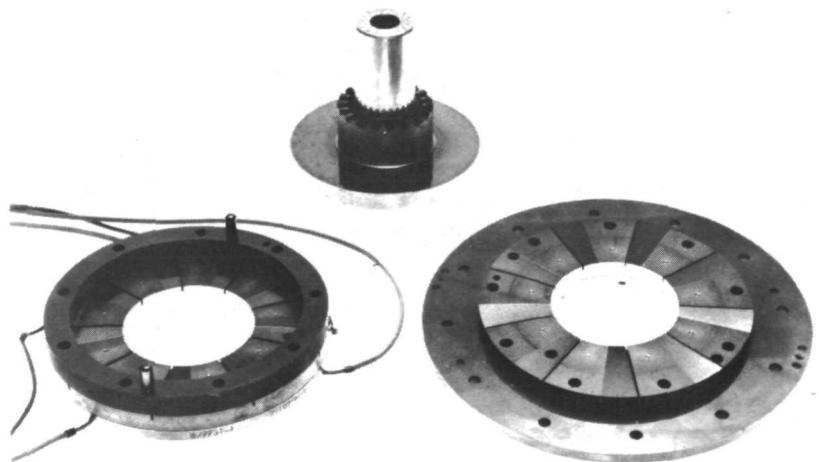
Figure 7. - Thrust stators and runner.
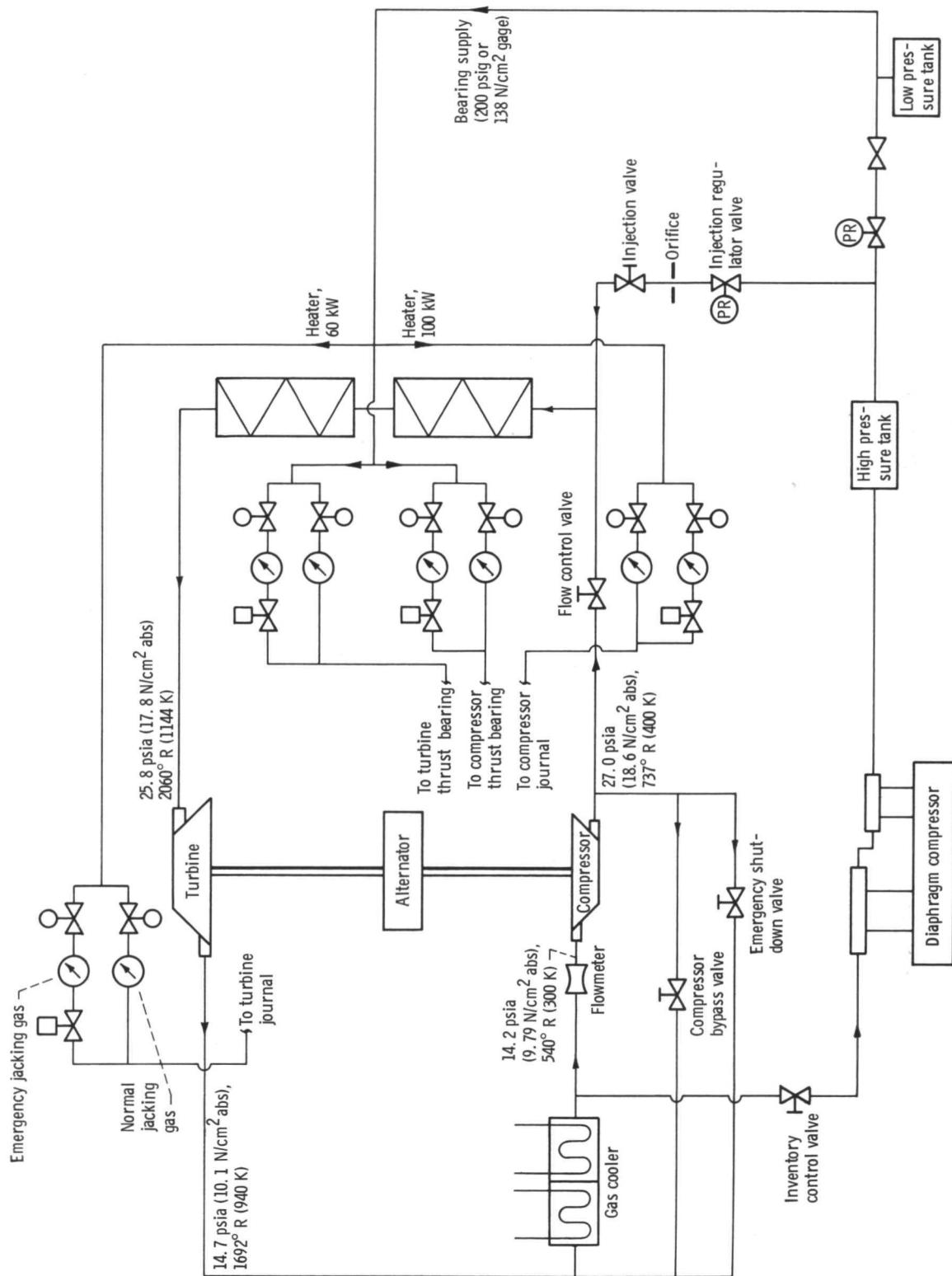
Figure 8. - Test loop schematic with 6-kilowatt design operating conditions.

Bearing supply (200 psig or 138 N/cm² gage)

Low pressure tank

CD-10520-15

Injection valve

Orifice

Injection regulator valve

High pressure tank

Heater, 60 kW

Heater, 100 kW

Flow control valve

To turbine thrust bearing

To compressor thrust bearing

To compressor journal

25.8 psia (17.8 N/cm² abs) 2060° R (1144 K)

27.0 psia (18.6 N/cm² abs), 737° R (400 K)

Turbine

Alternator

Compressor

Diaphragm compressor

Emergency jacking gas

Normal jacking gas

To turbine journal

14.7 psia (10.1 N/cm² abs), 1692° R (940 K)

14.2 psia (9.79 N/cm² abs), 540° R (300 K)

Flowmeter

Compressor bypass valve

Emergency shut-down valve

Gas cooler

Inventory control valve

24

(a) Control valve positions.

Figure 9. - Test facility operating conditions during startup.
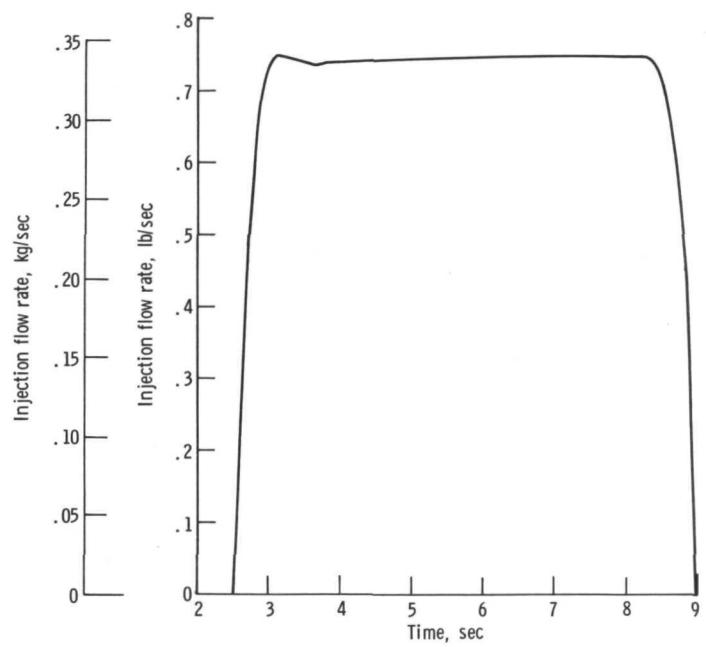
(b) Injection flow rate.

Figure 9. - Continued.
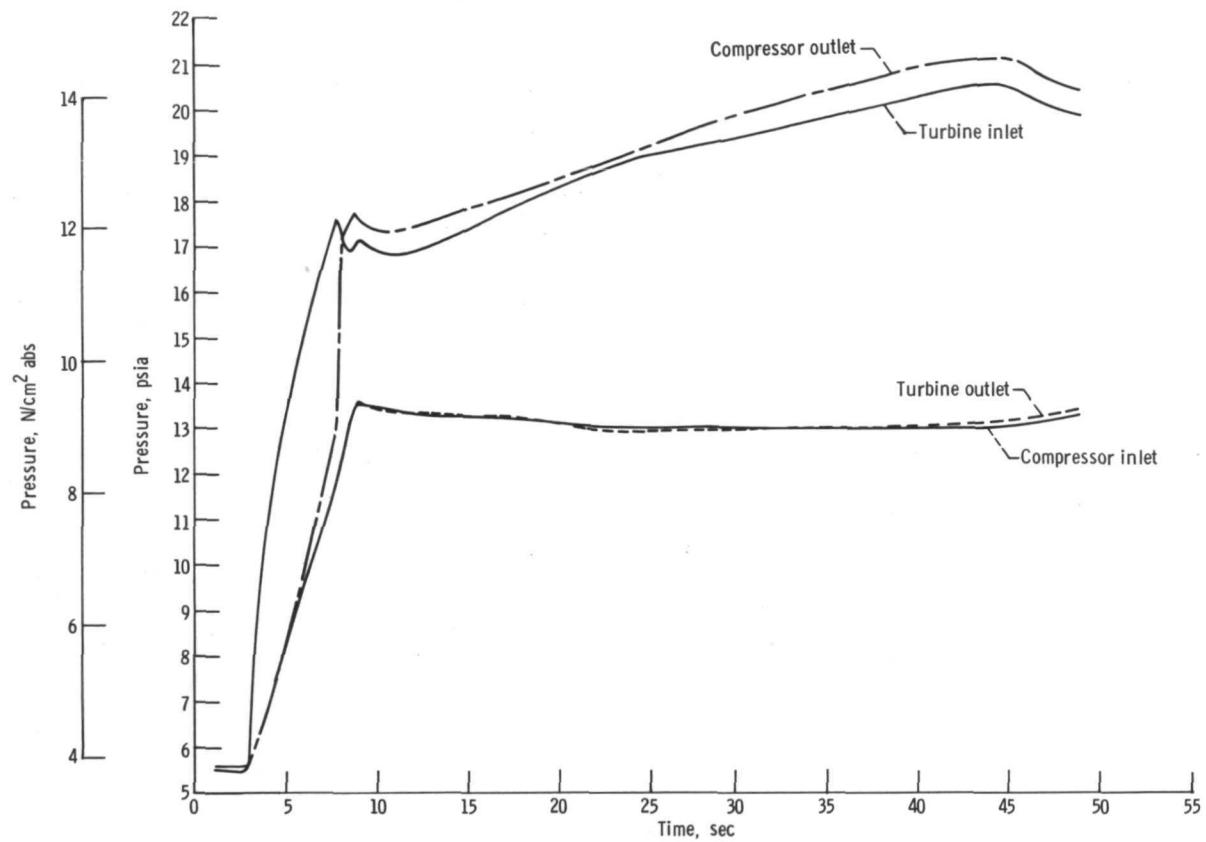
(c) Turbine and compressor total pressures.

Figure 9. - Continued.
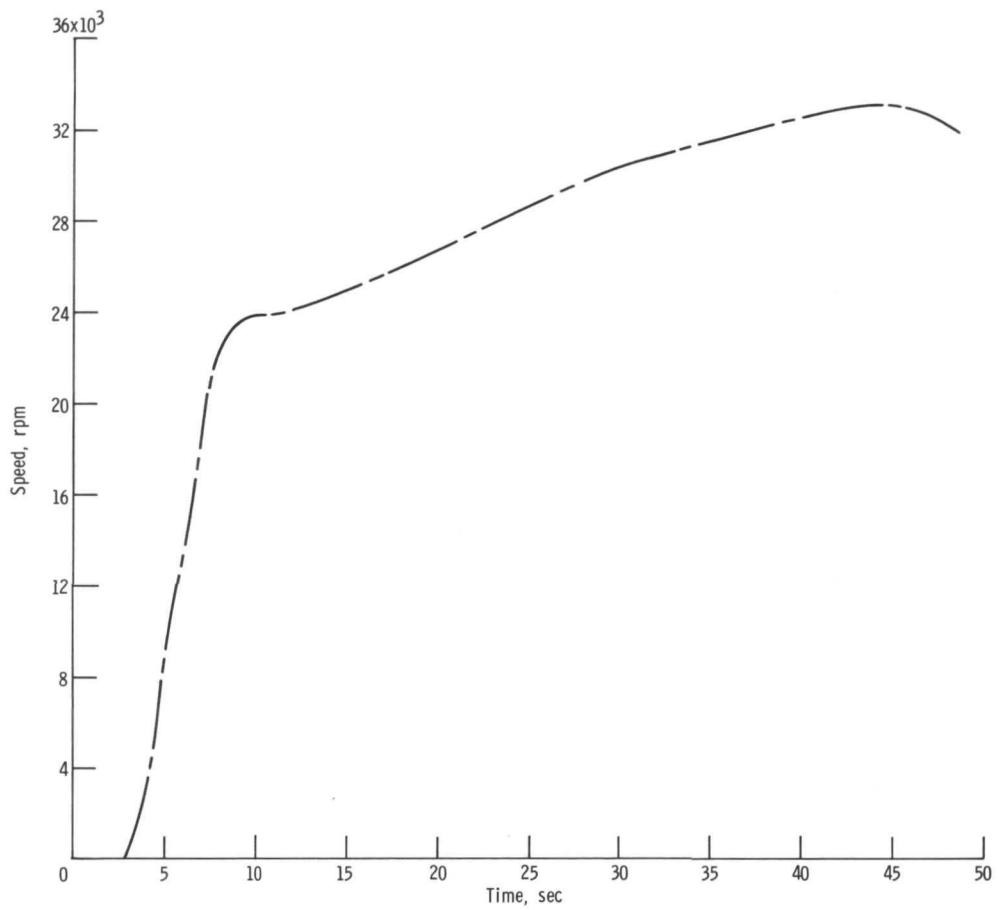
(d) Rotative speed.

Figure 9. – Continued.
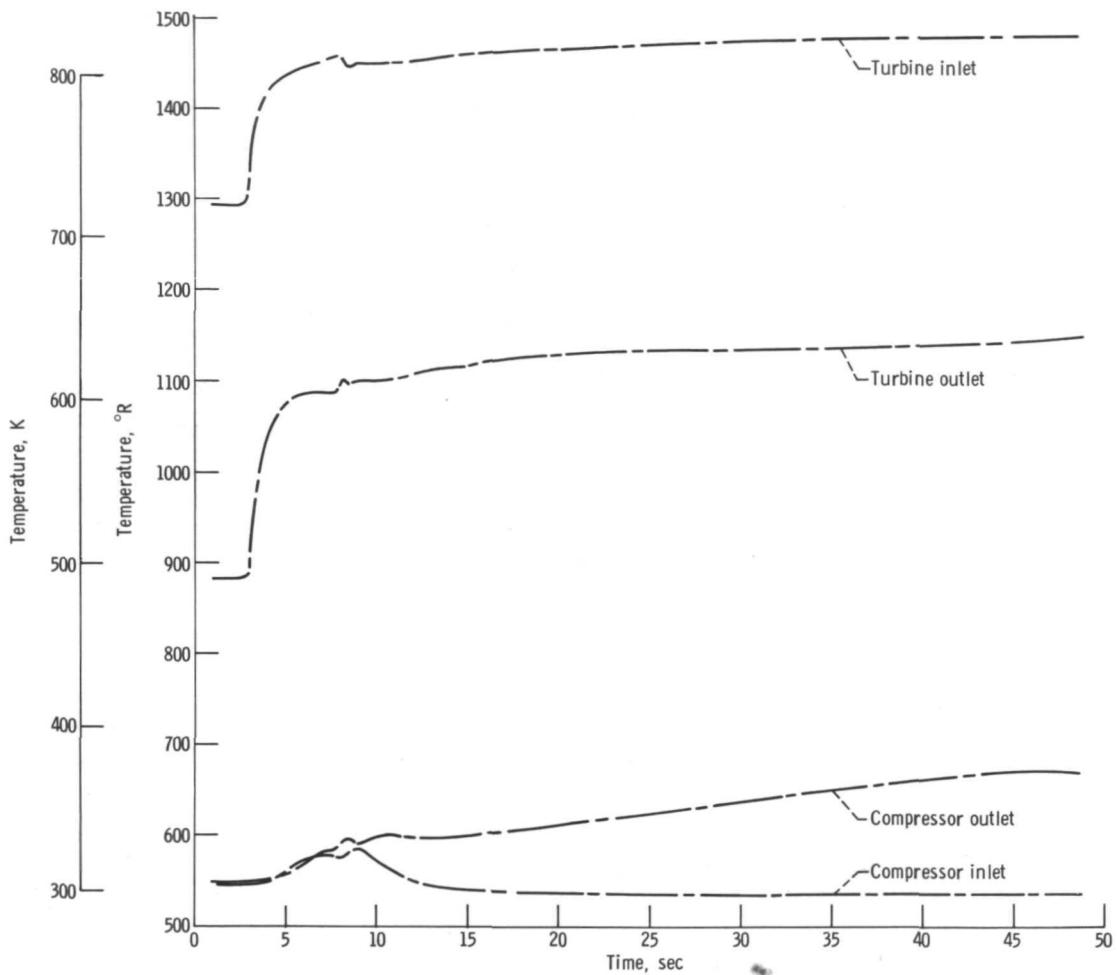
(e) Turbine and compressor total temperatures.

Figure 9. – Continued.
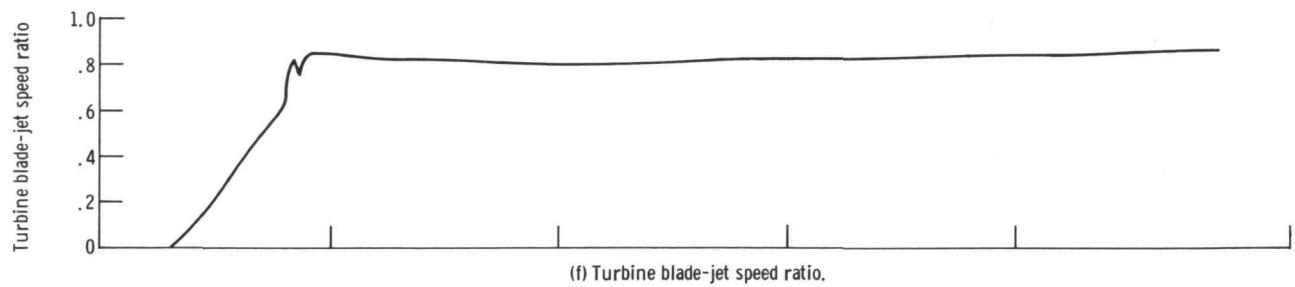
(f) Turbine blade-jet speed ratio.
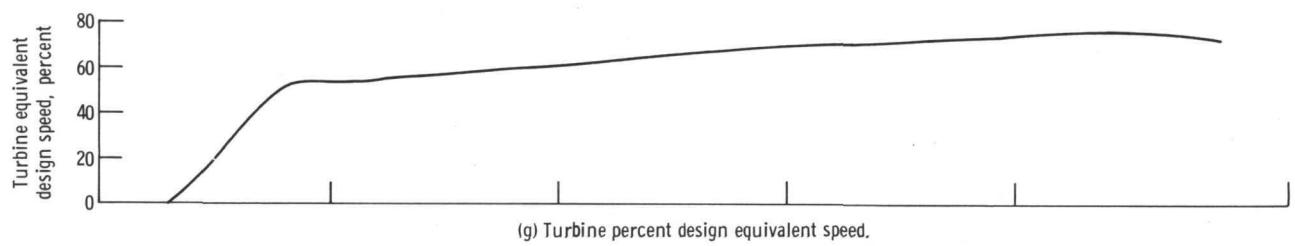
(g) Turbine percent design equivalent speed.
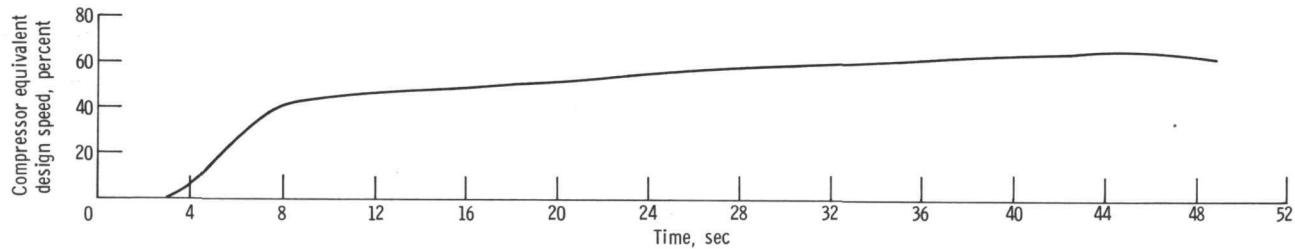
(h) Compressor percent design equivalent speed.

Figure 9. – Concluded.

Figure 10. - Location of thermocouples in BRU.

Thermocouple
39, Compressor outlet scroll
71, Turbine inlet scroll

CD-10521-15

31
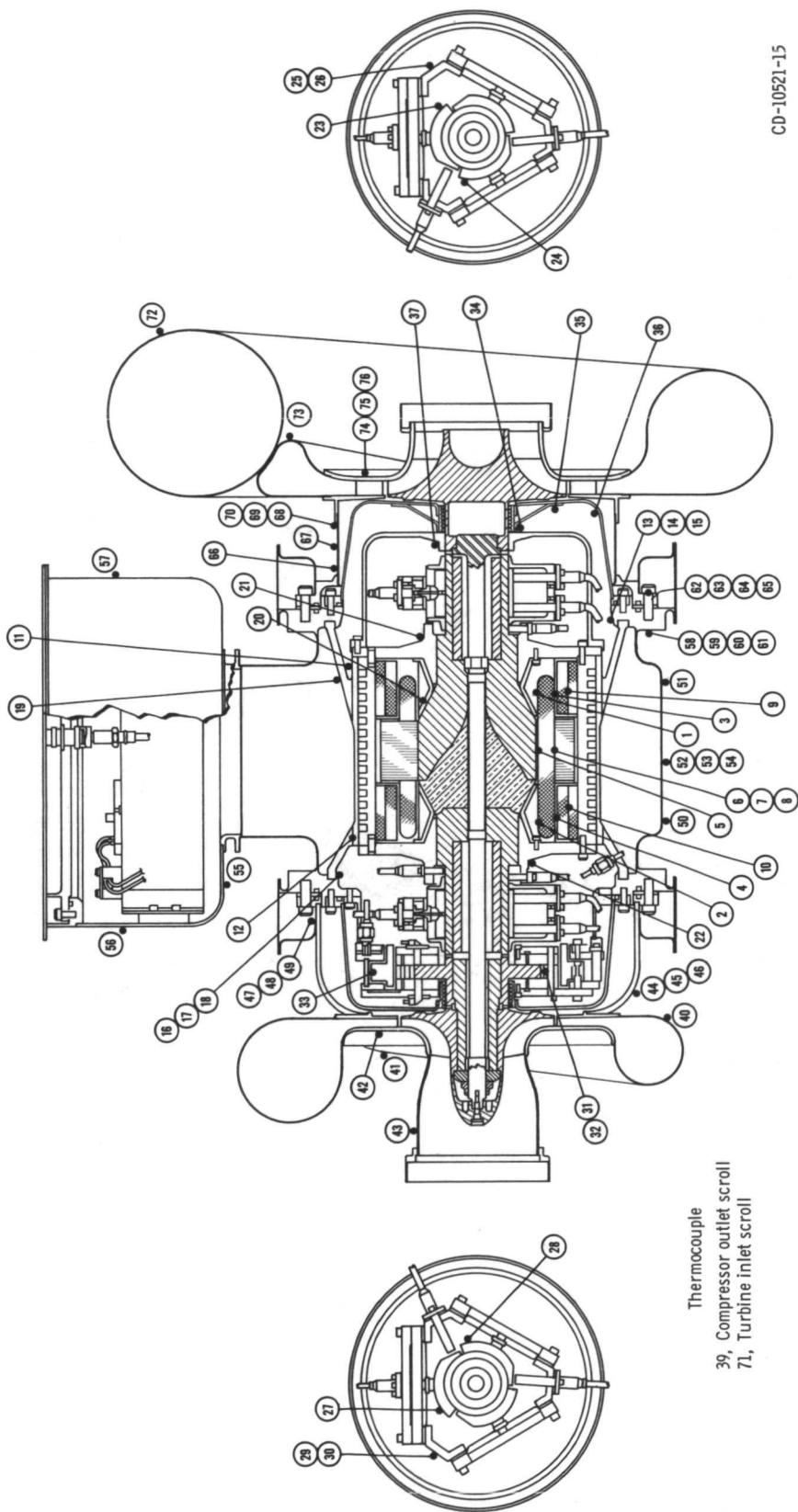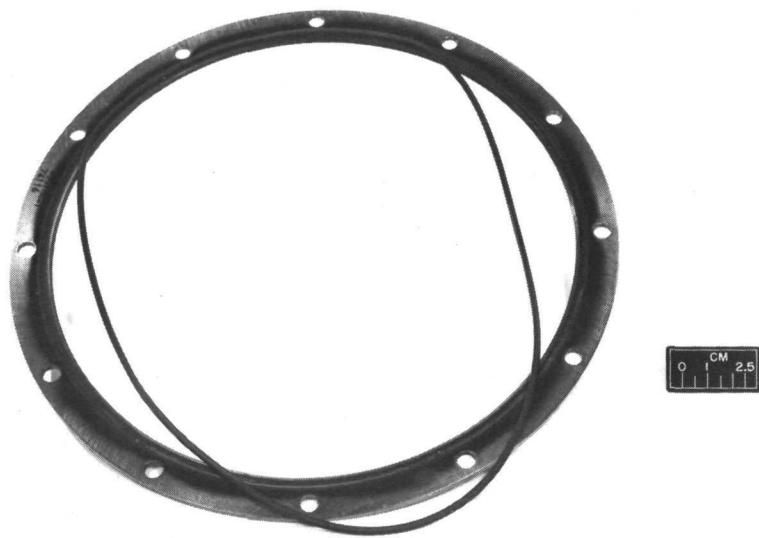
C-69-1069

Figure 11. - O-ring and spacer used to seal turbine scroll to housing.
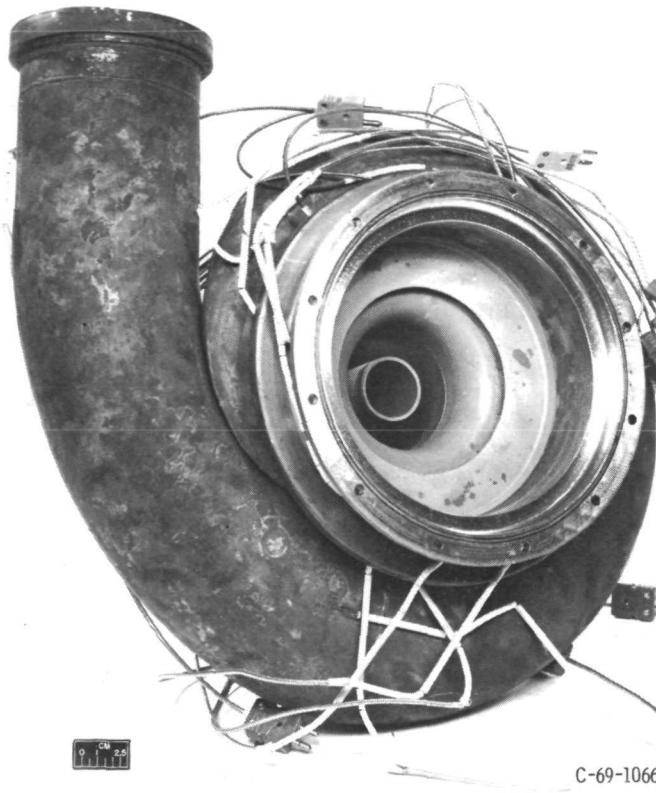
Figure 12. - Deterioration of gold reflective surfaces.

Figure 13. - Rhodium plated turbine seal holder.
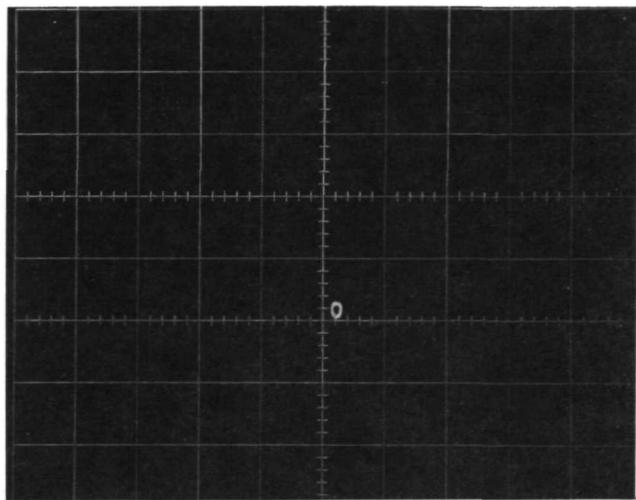
(a) Compressor journal bearing orbit.
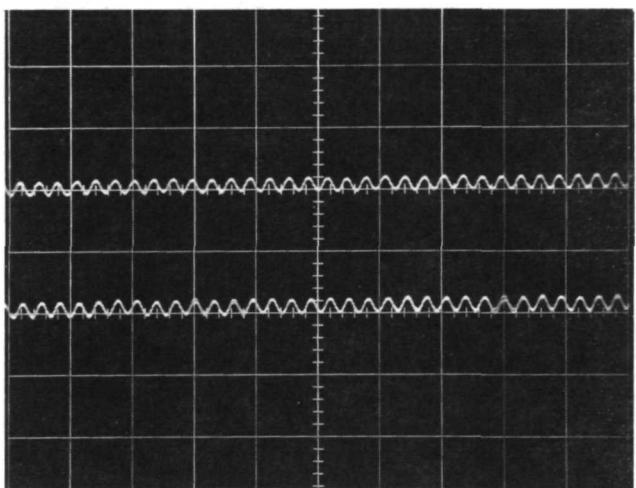
(b) Compressor journal bearing; orthogonal probes on time base.
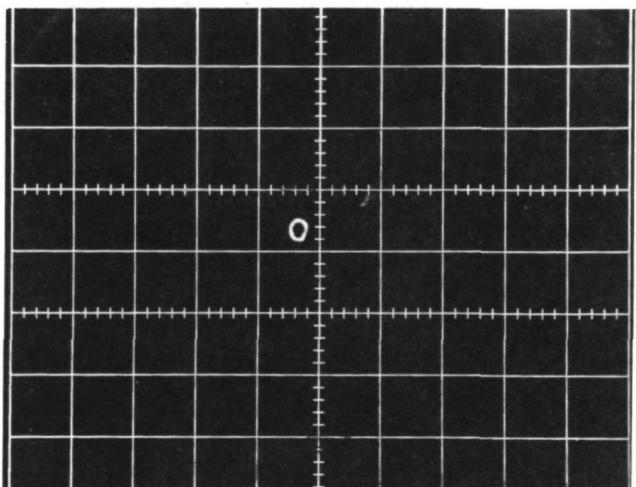

(c) Turbine journal bearing orbit.

Figure 14. - Oscilloscope traces of bearing component motions.
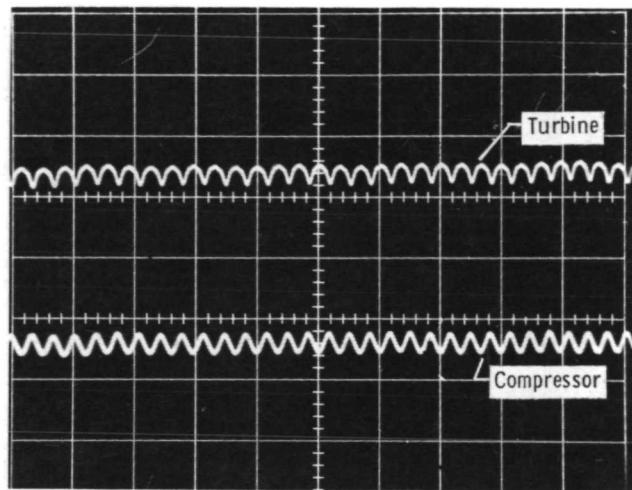
(g) Radial motions of turbine and compressor; flexibly mounted pivots.
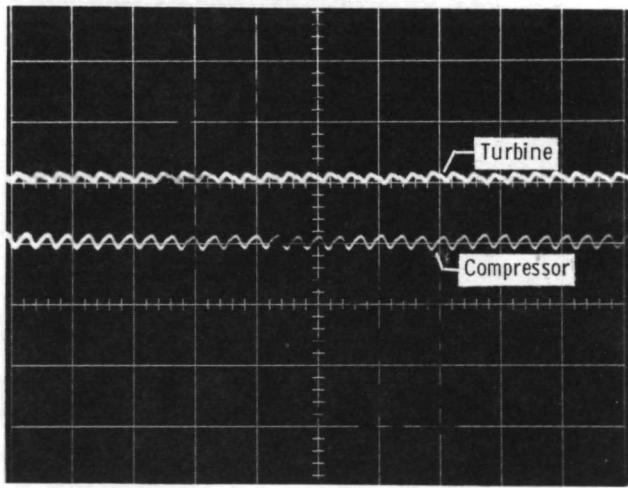

(h) Turbine and compressor end thrust.
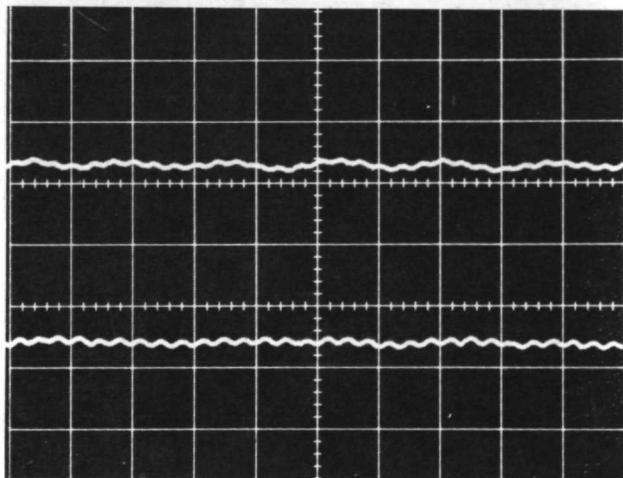

(i) Gimbal motions.

Figure 14. – Concluded.
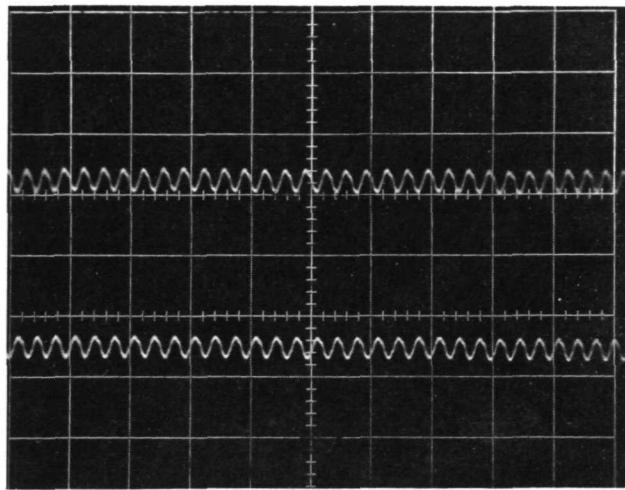
(d) Turbine journal bearing; orthogonal probes on time base.
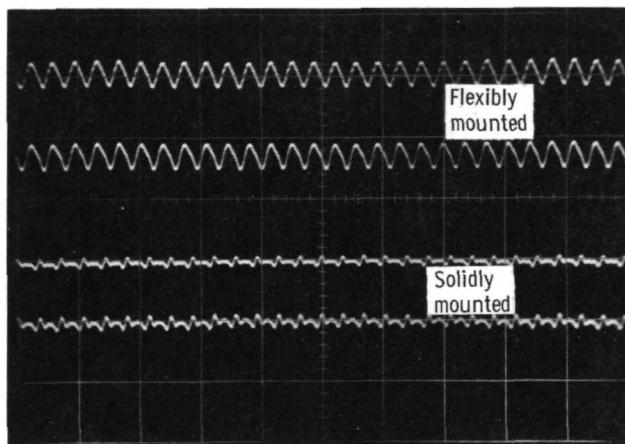
(e) Leading edge motions of turbine journal bearing; flexibly and solidly mounted pads.
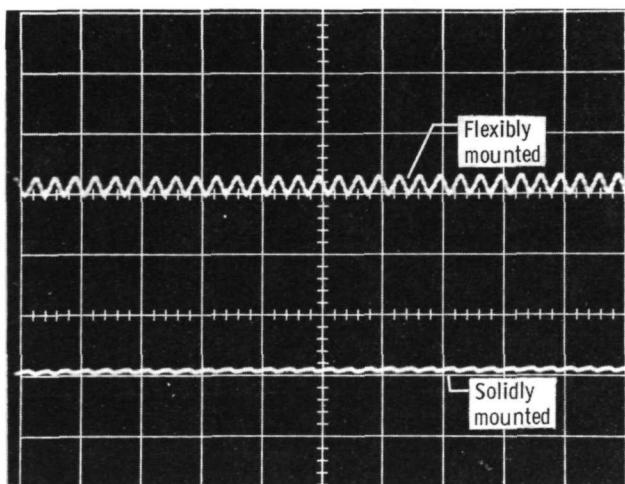
(f) Leading edge motions of compressor journal bearing; flexibly and solidly mounted pads.

Figure 14. - Continued.

E-5130

"The aeronautical and space activities of the United States shall be conducted so as to contribute . . . to the expansion of human knowledge of phenomena in the atmosphere and space. The Administration shall provide for the widest practicable and appropriate dissemination of information concerning its activities and the results thereof."

— NATIONAL AERONAUTICS AND SPACE ACT OF 1958

NASA SCIENTIFIC AND TECHNICAL PUBLICATIONS

TECHNICAL REPORTS: Scientific and technical information considered important, complete, and a lasting contribution to existing knowledge.

TECHNICAL NOTES: Information less broad in scope but nevertheless of importance as a contribution to existing knowledge.

TECHNICAL MEMORANDUMS: Information receiving limited distribution because of preliminary data, security classification, or other reasons.

CONTRACTOR REPORTS: Scientific and technical information generated under a NASA contract or grant and considered an important contribution to existing knowledge.

TECHNICAL TRANSLATIONS: Information published in a foreign language considered to merit NASA distribution in English.

SPECIAL PUBLICATIONS: Information derived from or of value to NASA activities. Publications include conference proceedings, monographs, data compilations, handbooks, sourcebooks, and special bibliographies.

TECHNOLOGY UTILIZATION PUBLICATIONS: Information on technology used by NASA that may be of particular interest in commercial and other non-aerospace applications. Publications include Tech Briefs, Technology Utilization Reports and Notes, and Technology Surveys.

Details on the availability of these publications may be obtained from:

SCIENTIFIC AND TECHNICAL INFORMATION DIVISION

NATIONAL AERONAUTICS AND SPACE ADMINISTRATION

Washington, D.C. 20546